Available online at www.sciencedirect.com

ScienceDirect

Ceramics International 40 (2014) 1171–1175

CERAMICS INTERNATIONAL

www.elsevier.com/locate/ceramint

Optical properties of multiferroic $LuFeO_3$ ceramics

L.P. Zhu[a], H.M. Deng[b], L. Sun[a], J. Yang[a], P.X. Yang[a,*], J.H. Chu[a]

[a]Key Laboratory of Polar Materials and Devices, Ministry of Education, Department of Electronics, East China Normal University, Shanghai 200241, PR China
[b]Laboratory for Microstructures, Shanghai University, 99 Shangda Road, Shanghai 200444, PR China

Received 28 April 2013; received in revised form 2 May 2013; accepted 1 July 2013
Available online 6 July 2013

Abstract

We report on the optical behavior of pure orthorhombic perovskite $LuFeO_3$ ceramics in the energy range of 1.24–5 eV determined by spectroscopic ellipsometry and diffuse reflectance spectroscopy. The value of optical band gap for the $LuFeO_3$ was confirmed to be 2.76 ± 0.01 eV. Main mechanism of $LuFeO_3$ ceramics for the band gap possibly arises from the direct electronic transitions between the major channel Fe 3d to O 2p (t_{1g} (π) to t_{2g}) charge transfer excitation.

Keywords: C. Optical properties; $LuFeO_3$; Spectroscopic ellipsometry; Diffuse reflectance spectroscopy

1. Intruduction

Multiferroic materials have attracted much attention for their abundant potential applications to modern optoelectronics and spintronics [1,2]. For the practical application, looking for the room temperature multiferroic materials is the urgent affairs. Materials showing occurrence of intrinsic multiferroism are rather rare. An interesting candidate for intrinsic multiferroism is $LuFeO_3$ [3–6]. The possible interaction in $LuFeO_3$ is different from that in original multiferroic compounds, and that will deeply affect the development of new spintronics and optoelectronics devices [2,7]. Furthermore, Zhang et al. [6] observed that a giant dielectric constant step with strong frequency dispersion in $LuFeO_3$ similar to that in $LuFe_2O_4$, Accompanied by its dielectric characteristic, this material possess particular properties, such as structural anisotropy and anti-symmetric spin coupling [8,9]. All of these advantages make $LuFeO_3$ a unique multiferroic material.

$LuFeO_3$, as a member of the rare-earth orthoferrites family, crystallize with the orthorhombic distorted perovskite structure in space group Pbnm. Both the oxygen environment of the Lu^{3+} cation and the octahedral environment of the Fe^{3+} ion are strongly distorted. The ions of transition metals in the compounds partially and even completely sometimes govern their optical, magnetic, and other properties [10]. Recently, there have been some reports on the optical properties and electronic structure of $LuFeO_3$. From the views of experimental, Wang et al. [11] investigated the optical spectra of hexagonal films of $LuFeO_3$, the optical band gap was assigned to 2.0 eV with crystal field energy splitting of Fe^{3+} and purely charge transfer theory. Pavlov et al. [12] studied optical absorption of hexagonal $RFeO_3$ (R = Ho, Er, Lu) films, the absorption bands were assigned to 2.27 and 2.97 eV. From the views of theoretical calculation, the band gap of $LuFeO_3$ has been studied by different groups [13], but nor have they reached consensus on it. However, the optical band gap (E_g) parameter of a given material is of particular importance for both scientific understandings and potential technological applications. And the previous studies of $LuFeO_3$ mostly focused on the films, few researches have been conducted on bulk form. In order to clarify and elaborate the optical properties of $LuFeO_3$, the further investigation of optical spectroscopy is believed to be crucial. In this work, ultraviolet–visible–near-infrared (UV–vis–NIR), diffuse reflectance spectroscopy (DRS) and spectroscopic ellipsometry (SE) were employed to identify the optical parameters of $LuFeO_3$ ceramics.

2. Experimental

$LuFeO_3$ ceramics were prepared by a routine solid state reaction method. Lu_2O_3 (99.99%) and Fe_2O_3 (99%) were used as raw

*Corresponding author.
E-mail address: pxyang@ee.ecnu.edu.cn (P.X. Yang).

0272-8842/$ - see front matter © 2013 Elsevier Ltd and Techna Group S.r.l. All rights reserved.
http://dx.doi.org/10.1016/j.ceramint.2013.07.001

materials. Stoichiometric amounts of the raw materials were weighed and wet milled for 5 h using absolute alcohol and zirconia balls, dried in a non-vacuum evaporator at 353 K. The dried powders were compressed into pellets and then pre-sintered at 1073 K for 2 h using a muffle furnace. The sintered pellets were ground into powder and finally calcined for 2 h at 1473 K in air to form the ceramic samples. The procedure was repeated to increase sample homogeneity. The samples were double-side polished with a mechanical polishing process to smooth the surface. This process consists of three procedures: coarse grinding, fine grinding, and polishing. Then, the ceramics were rigorously cleaned in pure ethanol with an ultrasonic bath and rinsed several times by deionized water for spectral measurements. The phase purity of the sintered ceramics was determined by X-ray diffraction (XRD, Rigaku D/max-2200, with Cu K_α radiation). The surface micrograph of the sintered samples was characterized by a field emission scanning electron microscopy (FESEM, Philips XL30FEG). Raman scattering experiment of the ceramic was performed with a micro-Raman spectrometer (Jobin-Yvon LabRAM HR 800UV, using the 488 nm emission line of argon ion laser). The ellipsometric measurements were carried out in the photon energy range of 1.24–5 eV (245–1000 nm) with a spectral resolution of 1.5 nm by UV–vis–NIR SE (M-2000 by J.A. WOOLLAM CO. INC.). UV–vis–NIR DRS of the ceramics was recorded on a Varian Cary 500 UV–vis–NIR spectrometer equipped with the integration sphere in the wavelength region between 200 and 2000 nm.

3. Results and discussion

X-ray diffraction (XRD) patterns recorded at room temperature of the $LuFeO_3$ ceramics sintered at 1473 K for 2 h is shown in Fig. 1. All reflections could be adequately indexed according to $LuFeO_3$ (ICDD-PDF # 74-1483) with orthorhombic perovskite structure. It indicates that the samples are pure perovskite structure and there are no additional or intermediate phases, which also can be confirmed by the following Raman spectroscopy. Lattice constants *a*, *b*, *c* and volume of unit cell for the $LuFeO_3$ ceramics by Bragg's law are 5.216 Å, 5.552 Å, 7.584 Å (magnitude of error, ± 0.001 Å) and 219.63 $Å^3$, respectively. In comparison with the standard data for $LuFeO_3$ powder crystals obtained from JCPDS # 74-1483, the lattice constants obtained here are slightly larger. There are two possible reasons for this change in lattice constants. One is grain clamping effect in process of formation of ceramics and the stress maintain vacancy defects found in grain boundary, the other is intrinsic vacancy defects caused by slight non-stoichiometry. The inset of Fig. 1 illustrates the SEM image of the sample sintered at 1473 K. It can be seen that there are many square-shaped grains stacking onto each other with the average grain size about 3 μm.

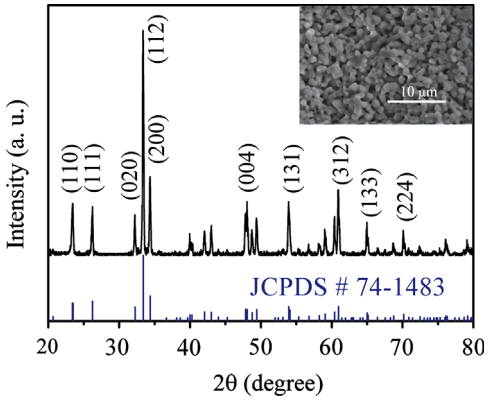

Fig. 1. X-ray diffraction pattern for $LuFeO_3$ ceramics sintered at 1473 K in air for 2 h. The inset is SEM micrograph of the surface of $LuFeO_3$ ceramics.

Fig. 2 shows the Raman spectra of polycrystalline $LuFeO_3$ ceramics, measured at room temperature using 488 nm excitation lines. Raman spectroscopy is also the powerful method to analyze the structure and the phase purity of the samples. In order to obtain the exact peaks, which represent the presence of Raman active modes, the measured spectra were fitted, and the fitted curves were decomposed into individual Lorentzian components, the peaks positions can be deduced, which are summarized in Table 1. There are four $LuFeO_3$ units within the unit cell, and the 12 oxygen atoms are distributed among sites of two different symmetries within the unit cell, as shown in inset of Fig. 2. Since there are 20 atoms in the primitive cell, the phonon dispersion relation has three acoustical and 57 optical phonon branches. The site symmetries of all the ions are as follows:

$$Lu^{3+}(Cs); Fe^{3+}(C_i); O_I^{2-}(Cs); O_{II}^{2-}(C_1).$$

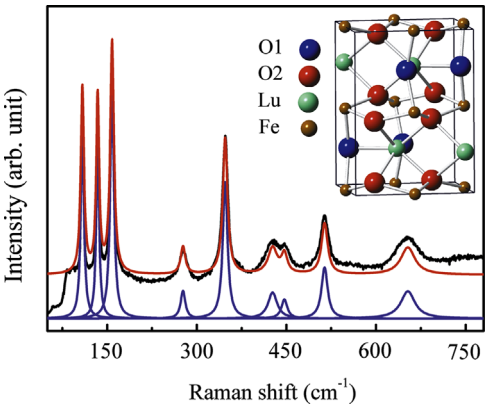

Fig. 2. Measured Raman spectra (black line), together with their fitted spectra (red line) and the decomposed active modes (violet line), for $LuFeO_3$. The unit cell of $LuFeO_3$ crystals is shown as inset. (For interpretation of the references to color in this figure legend, the reader is referred to the web version of this article.)

Table 1
Comparison of Raman peaks between experimental results and literature.

	Raman peak								
Our work (± 2 cm^{-1})	108	134	158	277	347	427	446	514	653
literature[a]	110	136	158	278	350	427	450	516	654
Phonon mode	A_g	A_g/B_{1g}	A_g	A_g/B_{1g}	A_g/B_{1g}	A_g/B_{1g}	A_g	A_g/B_{1g}	A_g

[a]Ref. [14].

Fe^{3+} ions possessing the inversion symmetry generate no Raman active mode. First order Raman scattering is expected from 24 active modes with the representations A_{1g}, B_{1g}, B_{2g} and B_{3g} [14]. Only nine modes could be detected here. The other modes (B_{2g} and B_{3g}) probably exhibit either too weak intensities or have frequencies outside the measured spectral range. Furthermore, it should be noted that also for other perovskite oxides belonging to the Pnma space group, e.g. $LaMnO_3$, $BiCrO_3$ [15–17], a smaller number of modes than theoretically predicted were observed experimentally. As shown in Table 1, the peak positions are in good agreement with the previous measurements in a single crystal of $LuFeO_3$ [14], further indicating that the $LuFeO_3$ sample with pure orthorhombic pervoskite phase.

As a sensitive and nondestructive optical method, SE based on the reflectance configuration is easily acceptable for the determination of optical constants [18]. In order to extract the optical function from the ellipsometric spectra, a dielectric function model should be applied. The optical properties of the $LuFeO_3$ ceramics are analyzed via fitting the reflectance spectra with reasonable dielectric function model. The complex reflectance ratio, ρ, of ceramics is a function of ellipsometry parameters of Ψ and Δ. The fundamental equation of ellipsometric is described as: $\rho=\tan\Psi\exp(i\Delta)$. The dielectric function (ε) of ceramic bulk is a common representation via the two-phase (air/ceramic) model [19,20],

$$\varepsilon=\varepsilon_1+i\varepsilon_2=\sin^2\phi+\sin^2\phi\tan^2\phi\frac{(1-\rho)^2}{(1+\rho)^2},$$

where φ is the angle of incidence, ρ is the complex reflectance ratio. The diectric functions are related to the refractive index, n, and extinction coefficient, k, by the Fresnel formula: $\varepsilon_1=n^2-k^2$, and $\varepsilon_2=2nk$.

Fig. 3 shows the experimental ellipsometric data (Ψ and Δ) for the $LuFeO_3$ ceramic from near-infrard to ultraviolet photon energy region recorded at the incident angle of 70°. Inset of Fig. 3 shows the calculations of refractive index (n) and extinction coefficient (k). Bahng et al. [21], Shen et al. [22], and Chu et al. [23] proposed that the values of refractive index peaks generally correspond to the band gap energies of the dielectrics and semiconductors. This can be understood from the Kramers–Kronig relation,

$$n(\nu)=1+\frac{c}{\pi}\int_0^\infty\frac{d\alpha(\nu')}{\nu'}\log\left(\frac{\nu'+\nu}{\nu'-\nu}\right)d\nu'$$

where c is the light velocity, ν' and ν are frequencies of light, and $\alpha(\nu')$ is the absorption coefficient at frequency ν'. In the energy region near the fundamental absorption region, the value of $d\alpha(\nu')/d\nu'$ goes up and the refractive index increases as the photon energy enhances. However, when the photon energy reaches the gap energy, i.e., interband critical point, the absorption curve changes its slope and becomes flatter, and then the value of $d\alpha(\nu')/d\nu'$ decreases above the gap energy. Thus, peaks appear in the refractive index at the gap energy. The refractive index peak site is 2.78 eV. This value is in good agreement with the values determined by Tauc's power law, and it is also similar to the other perovskite oxides, e.g. $BiFeO_3$ (Ref. 2).

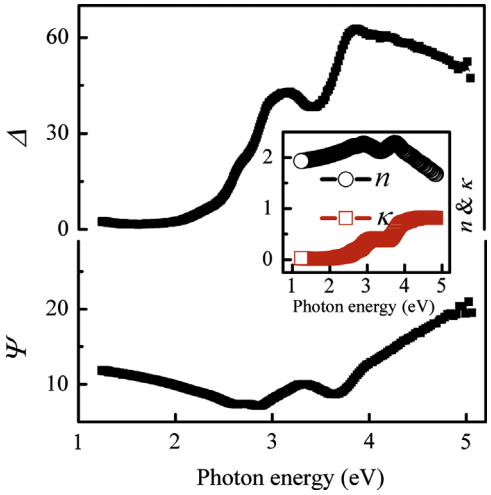

Fig. 3. Experimental ellipsometric data (Ψ and Δ) for the $LuFeO_3$ ceramic from near-infrard to ultraviolet photon energy region recorded at the incident angle of 70°. The inset shows the refractive index, n, and extinction coeffient, κ.

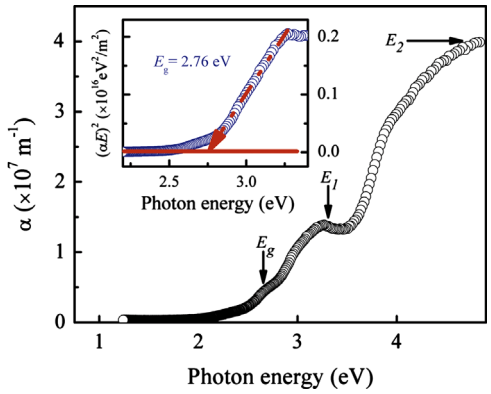

Fig. 4. Optical absorption coefficient α of $LuFeO_3$ ceramic. The inset shows E_g determination by Tauc's power law.

Fig. 4 shows the absorption coefficient ($\alpha=4\pi\kappa/\lambda$) as a function of photon energy ($h\nu$). It can readily identified two features at about 3.3 eV (E_1) and 4.7 eV (E_2). We demonstrate that the absorption coefficient in the spectral region around E_1 and E_2 is extremely large, with values of α in excess of $10^7\ m^{-1}$. This should compare to the values of 10^2–$10^6\ m^{-1}$ in the spectral region immediately above the optical gap [11]. The band edge absorption is completely negligible on the scale of the data because of the band edge absorption is weak and the density of states at the band edge is comparatively small [24–26]. Thus, the optical gap of $LuFeO_3$ should be located around E_g region (2–3 eV). The optical gap, E_g, values of the $LuFeO_3$ ceramics can be evaluated from Tauc's power law, $\alpha E\propto(E-E_g)^\eta$, where $E=h\nu$ the photon energy, and η is a constant with value 1/2 for a direct band gap type and 2 for an indirect one. Inset of Fig. 4 shows a plot of $(\alpha E)^2$ ($\eta=1/2$) versus photon energy. The extrapolated linear portions show that the optical gap for direct transition is 2.76 ± 0.01 eV.

To better explain electronic structure of the orthorhombic $LuFeO_3$, the DRS measurement was performed. Fig. 5 shows the DRS absorbance spectra of the $LuFeO_3$ ceramics. It can be easily found two evident peaks at 1.22 and 1.73 eV, and a steep

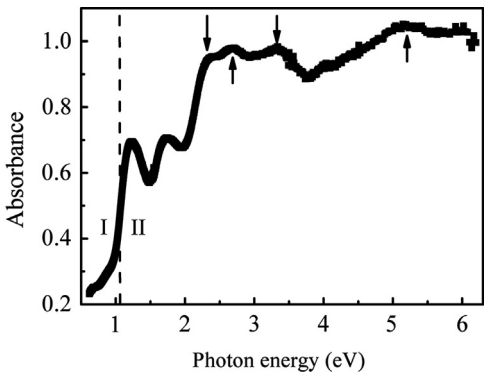

Fig. 5. Optical absorption spectra of the $LuFeO_3$ ceramic using diffuse reflectance spectroscopy.

slope around 1 eV, not similar to the reported optical properties of hexagonal $LuFeO_3$ films. This discrepancy is due to the form of material and characterization methods. The origin of the peaks detected in the sample could be manifold. We analyze the possible origin of the observed absorption bands here on the basis of crystal filed theory and charge transfer transition. The spectra can be roughly divided by the dashed line into two parts. The first part (I) is called as Drude region, and the other one (II) is the charge transfer (CT) region [27]. Valence shell structures of Lu, Fe, and O are $5s5p5d4d6s$, $3s3p4s4p3d$, and $2s2p$ states, respectively [13]. $LuFeO_3$ has a simple magnetic structure because of the complete f shell of lutetium. One Fe^{3+} contains five $3d$ electrons, which reside in a high spin state and occupy the only spin sextet and orbital singlet ^6S lying below the other terms [10]. There are 18 oxygen O $2p$ atomic orbitals in the octahedral FeO_6. The results of the evident peak position are in good agreement with the literatures [10]. 1.22 and 1.73 eV are the transitions from $^6A_{1g}$ to $^4T_{1g}$ and $^4T_{2g}$ split line, respectively, which can be summarized to crystal field d–d transitions [2,10]. There are also four broad peaks at 2.34, 2.73, 3.35 and 5.14 eV marked by the arrows in Fig. 5. The local charge transfer energy to move an electron from the O^{2-} ion to the Fe^{3+} ion is essentially given by the difference in the ionization potential of O and the electron affinity of Fe in the actual solid [28]. Thus, the electron excitation around 5.14 eV is probably strong hybridized major channel O $2p$ and Fe $3d$ to Lu $5d$ state excitation. The low-energy intense band around 3.35 eV can be assigned to the strong dipole-allowed on-center $t_{2\mu}$ (π) to t_{2g} p–d CT transition as in literature [29]. Possible mechanisms for the inflection points at 2.34 is Fe^{3+} d–d crystal field transition, and points at 2.73 eV is the optical band gap, possibly the major channel Fe $3d$ to O $2p$ (t_{1g} (π) to t_{2g}) charge transfer excitation. This result of optical band gap of DRS measurement was further explained with the previous SE investigation. Furthermore, defect and slight non-stoichiometry in the sample might ascribe to the broad peak in the spectral, and this requires a more thorough investigation, especially by high resolution electron microscopy.

4. Conclusions

In conclusion, XRD and Raman scattering results show that $LuFeO_3$ ceramics sintered at 1473 K for 2 h possesses orthorhombic perovskite structure. The optical band gap for $LuFeO_3$ is 2.76 ± 0.01 eV by Tauc's power law. The value of refractive index peak is 2.78 eV generally correspond to the band gap energies. The detailed electronic transitions of multiferroic $LuFeO_3$ have been further investigated using UV–vis diffuse reflectance spectroscopy, and the band gap obtained by DRS is 2.73 eV.

Acknowledgments

We thank Dr. Kai Jiang, Professor Zhigao Hu for technical support of the SE and Raman scattering spectra experiments. This work was financially supported by the National Natural Science Foundation of China (60990312, 61076060 and 11104074) and Science and Technology Commission of Shanghai Municipality 10JC1404600 and 11ZR1410800).

References

[1] W. Eerenstein, N.D. Mathur, J.F. Scott, Multiferroic and magnetoelectric materials, Nature 442 (2006) 759–765.
[2] R.V. Pisarev, A.S. Moskvin, A.M. Kalashnikova, T. Rasing, Charge transfer transitions in multiferroic $BiFeO_3$ and related ferrite insulators, Physical Review B 79 (2009) 235128.
[3] Y. Qin, X.Q. Liu, X.M. Chen, Dielectric, ferroelectric and magnetic properties of Mn-doped $LuFeO_3$ ceramics, Journal of Applied Physics 113 (2013) 044113.
[4] E. Magome, C. Moriyoshi, Y. Kuroiwa, A. Masuno, H. Inoue, Non-centrosymmetric structure of $LuFeO_3$ in metastable state, Japanese Journal of Applied Physics 49 (2010) 09ME06.
[5] A.R. Akbashev, A.S. Semisalova, N.S. Perov, A.R. Kaul, Weak ferromagnetism in hexagonal orthoferrites $RFeO_3$ (R = Lu, Er–Tb), Applied Physics Letters 99 (2011) 122502.
[6] L. Zhang, X.M. Chen, Dielectric relaxation in $LuFeO_3$ ceramics, Solid State Communications 149 (2009) 1317–1321.
[7] N.A. Spaldin, M. Fiebig, The renaissance of magnetoelectric multiferroics, Science 309 (2005) 391–392.
[8] W.K. Zhu, L. Pi, S. Tan, Y.H. Zhang, Anisotropy and extremely high coercivity in weak ferromagnetic $LuFeO_3$, Applied Physics Letters 100 (2012) 052407.
[9] A. Masuno, S. Sakai, Y. Arai, H. Tomioka, F. Otsubo, H. Inoue, C. Moriyoshi, Y. Kuroiwa, J.D. Yu, Structure and physical properties of metastable hexagonal $LuFeO_3$, Ferroelectrics 378 (2009) 169–174.
[10] P.A. Usachev, R.V. Pisarev, A.M. Balbashov, A.V. Kimel, A. Kirilyuk, T. Rasing, Optical properties of thulium orthoferrite $TmFeO_3$, Physics of the Solid State 47 (2005) 2292–2298.
[11] W.B. Wang, H.W. Wang, X.Y. Xu, L.Y. Zhu, L.X. He, E. Wills, X. M. Cheng, D.J. Keavney, J. Shen, X.F. Wu, X.S. Xu, Crystal field splitting and optical band gap of hexagonal $LuFeO_3$ films, Applied Physics Letters 101 (2012) 241907.
[12] V.V. Pavlov, A.R. Akbashev, A.M. Kalashnikova, V.A. Rusakov, A. R. Kaul, M. Bayer, R.V. Pisarev, Optical properties and electronic structure of multiferroic hexagonal orthoferrites $RFeO_3$ (R = Ho, Er, Lu), Journal of Applied Physics 111 (2012) 056105.
[13] D.J. Adams, B. Amadon, Study of the volume and spin collapse in orthoferrite $LuFeO_3$ using LDA+U, Physical Review B 79 (2009) 115114.
[14] S. Venugopalan, M.M. Becker, Raman scattering study of $LuFeO_3$, Journal of Chemical Physics 93 (1990) 3833–3836.
[15] M.N. Iliev, M.V. Abrashev, Raman phonons and Raman Jahn–Teller bands in perovskite-like manganites, Journal of Raman Spectroscopy 32 (2001) 805–811.
[16] M.N. Iliev, M.V. Abrashev, J. Laverdière, S. Jandl, M.M. Gospodinov, Y.Q. Wang, Y.Y. Sun, Distortion-dependent Raman spectra and mode

mixing in $RMnO_3$ perovskites (R=La, Pr, Nd, Sm, Eu, Gd, Tb, Dy, Ho, Y), Physical Review B 73 (2006) 064302.
[17] C. Himcinschi, I. Vrejoiu, T. Weißbach, K. Vijayanandhini, A. Talkenberger, Raman spectra and dielectric function of $BiCrO_3$: experimental and first-principles studies, Journal of Applied Physics 110 (2011) 073501.
[18] P.X. Yang, M. Guo, M.R. Shi, X.J. Meng, Z.M. Huang, J.H. Chu, Spectroscopic ellipsometry of $SrBi_2Ta_{2-x}Nb_xO_9$ ferroelectric thin films, Journal of Applied Physics 97 (2005) 106106.
[19] S.K. Loyalka, C.A. Riggs, Inverse problem in diffuse reflectance spectroscopy: accuracy of the Kubelka–Munk equations, Applied Spectroscopy 49 (1995) 1107.
[20] R.M.A. Azzam, N.M. Bashara, Ellipsometry and Polarized Light, North-Holland, Amsterdam, 1977.
[21] J.H. Bahng, M. Lee, H.L. Park, I.W. Kim, J.H. Jeong, K.J. Kim, Spectroscopic ellipsometry study of $SrBi_2Ta_2O_9$ ferroelectric thin films, Applied Physics Letters, 79 (2001) 1664.
[22] L.F. Jiang, W.Z. Shen, H. Ogawa, Q.X. Guo, Temperature dependence of the optical properties in hexagonal AlN, Journal of Applied Physics 94 (2003) 5704.
[23] J.H. Chu, A. Sher, Physics and Properties of Narrow Gap Semiconductors, Springer, New York, 2008.
[24] M. Fox, Optical Properties of Solids, Oxford University Press, Beijing, 2009.
[25] K. Liu, J.H. Chu, D.Y. Tang, Composition and temperature dependence of the refractive index in $Hg_{1-x}Cd_xTe$, Journal of Applied Physics 75 (1994) 4176.
[26] J.H. Chu, S.C. Xu, D.Y. Tang, Energy gap versus alloy composition and temperature in $Hg_{1-x}Cd_xTe$, Applied Physics Letters 43 (1983) 1064.
[27] T. Arima, Y. Tokura, J.B. Torrance, Variation of optical gaps in perovskite-type 3d transition-metal oxides, Physical Review B 48 (1993) 17006–17009.
[28] J. Zaanen, G.A. Sawatzky, J.W. Allen, Band gaps and electronic structure of transition-metal compounds, Physical Review Letters 55 (1985) 418–421.
[29] F.J. Kahn, P.S. Pershan, J.P. Remeika, Ultraviolet magneto-optical properties of single-crystal orthoferrites, garnets, and other ferric oxide compounds, Physical Review 186 (1969) 891–918.